

AD-A051 315

NAVAL OCEAN SYSTEMS CENTER SAN DIEGO CA  
DETECTION OF SINUSOIDS IN UNCORRELATED NOISE USING ADAPTIVE LIN--ETC(U)  
JAN 78 S T ALEXANDER, J R ZEIDLER  
NOSC/TR-197

F/G 9/3

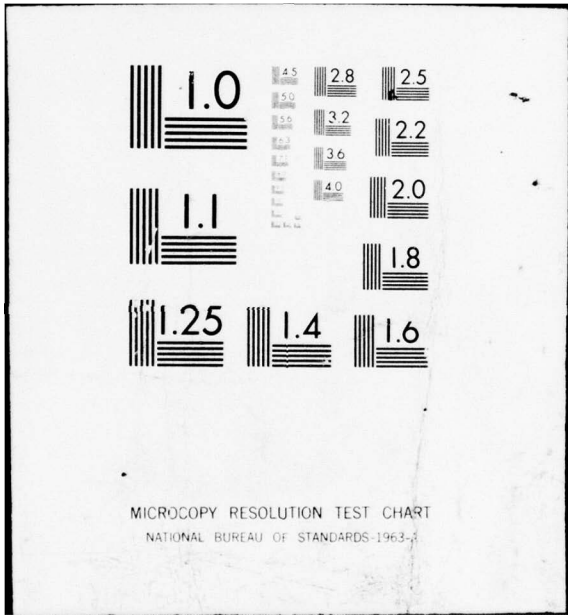
UNCLASSIFIED

NL

| OF |  
AD  
A051 315



END  
DATE  
FILMED  
-4-78  
DDC



AD A 051315

NOSC TR 197

# NOSC

12 2

NOSC TR 197

Technical Report 197

## DETECTION OF SINUSOIDS IN UNCORRELATED NOISE USING ADAPTIVE LINEAR PREDICTION FILTERS

ST Alexander  
JR Zeidler

31 January 1978

DDC  
RECEIVED  
MAR 16 1978  
RESERVED  
F

Final Report: March to September 1977

Prepared For  
Naval Electronic Systems Command

AD No. \_\_\_\_\_  
DDC FILE COPY

Approved for public release; distribution unlimited

NAVAL OCEAN SYSTEMS CENTER  
SAN DIEGO, CALIFORNIA 92152



NAVAL OCEAN SYSTEMS CENTER, SAN DIEGO, CA 92152

---

AN ACTIVITY OF THE NAVAL MATERIAL COMMAND

**RR GAVAZZI, CAPT, USN**

Commander

**HL BLOOD**

Technical Director

### ADMINISTRATIVE INFORMATION

The work covered in this report was done by the authors during fiscal year 1977 in the Fleet Engineering Department, Naval Ocean Systems Center and at ORINCON, San Diego. This work was sponsored by Code 320, Naval Electronic Systems Command.

Released by  
R H HEARN, Head  
Electronics Division

Under authority of  
D A KUNZ, Head  
Fleet Engineering Department

UNCLASSIFIED

SECURITY CLASSIFICATION OF THIS PAGE (When Data Entered)

REPORT DOCUMENTATION PAGE		READ INSTRUCTIONS BEFORE COMPLETING FORM	
1. REPORT NUMBER NOSC/TR-197	2. GOVT ACCESSION NO.	3. RECIPIENT'S CATALOG NUMBER	4. TYPE OF REPORT & PERIOD COVERED Technical report Research March-September 1977
5. TITLE (and Subtitle) DETECTION OF SINUSOIDS IN UNCORRELATED NOISE USING ADAPTIVE LINEAR PREDICTION FILTERS	6. PERFORMING ORG. REPORT NUMBER	7. AUTHOR(s) S. T. Alexander J. R. Zeidler	8. CONTRACT OR GRANT NUMBER(s)
9. PERFORMING ORGANIZATION NAME AND ADDRESS Naval Ocean Systems Center San Diego, California 92152	10. PROGRAM ELEMENT PROJECT, TASK AREA & WORK UNIT NUMBERS 62611 N F11101 XE1110100	11. CONTROLLING OFFICE NAME AND ADDRESS Naval Electronic Systems Command Washington, DC	12. REPORT DATE 31 January 1978
14. MONITORING AGENCY NAME & ADDRESS (if different from Controlling Office)	15. SECURITY CLASS. (of this report) Unclassified	13. NUMBER OF PAGES 25	15a. DECLASSIFICATION DOWNGRADING SCHEDULE
16. DISTRIBUTION STATEMENT (of this Report) Approved for public release; distribution unlimited.			
17. DISTRIBUTION STATEMENT (of the abstract entered in Block 20, if different from Report) D D C RECEIVED MAR 16 1978 F			
18. SUPPLEMENTARY NOTES			
19. KEY WORDS (Continue on reverse side if necessary and identify by block number) Adaptive line enhancer (ALE) Detection theory Receiver operating characteristics			
20. ABSTRACT (Continue on reverse side if necessary and identify by block number) This paper evaluates the detection performance of an application of adaptive linear prediction filtering known as the adaptive line enhancer (ALE) for the signal known except for phase problem. ROC curves are derived for an L-weight ALE followed by a K-point DFT under the conditions that $K \leq L$ and that K and L are much less than N, the total number of data points processed. ROC curves are also obtained for detection based on an L-point DFT of the L adaptive filter weights. It is shown that both ALE implementations give detection			

DD FORM 1 JAN 73 1473 EDITION OF 1 NOV 65 IS OBSOLETE

UNCLASSIFIED

SECURITY CLASSIFICATION OF THIS PAGE (When Data Entered)

next page

cm =

393 159

JOB

UNCLASSIFIED

SECURITY CLASSIFICATION OF THIS PAGE(When Data Entered)

20. (continued)

performances roughly comparable to N/L incoherent averages of an L-point DFT, but differences between the two ALE devices are noted. ALE detection performance is shown to be relatively insensitive to the choice of adaptive filter time constant. It is also shown that ALE detection performance is relatively insensitive to the value of K for  $K \leq L$ .

ACCESSION for	
NTIS	White Section <input checked="" type="checkbox"/>
DDC	Buff Section <input type="checkbox"/>
UNANNOUNCED	<input type="checkbox"/>
JUSTIFICATION	
BY	
DISTRIBUTION/AVAILABILITY CODES	
or	SPECIAL
A	

UNCLASSIFIED

SECURITY CLASSIFICATION OF THIS PAGE(When Data Entered)

## CONTENTS

INTRODUCTION	3
ADAPTIVE LINE ENHANCER (ALE) PERFORMANCE FOR SINUSOIDAL INPUTS IN WHITE NOISE	5
DERIVATION OF DETECTION STATISTICS	8
Detection Statistics for the ALE Output Device	8
Detection Statistics of the ALE Weight Vector Implementation	11
Detection Statistics for Incoherently Averaged DFT Processor	12
PERFORMANCE ANALYSIS	12
SUMMARY	17
REFERENCES	18
APPENDIX A	21
APPENDIX B	24

## ILLUSTRATIONS

1. Adaptive detector implementations	4
2. SNR at 50 percent $P_D$ as a function of optimal $\mu_0$ . $K = L$ , $P_{FA} = 10^{-4}$	13
3. ROC curves for $P_{FA} = 10^{-4}$ , $N = 102,400$ . $K = L = 1024$ , $\mu c^2 = 4.1 \times 10^{-6}$	14
4. ROC curves for $P_{FA} = 10^{-4}$ , $N = 12,800$ . $K = L = 128$ , $\mu c^2 = 3 \times 10^{-5}$	15
5. ROC curves for $P_{FA} = 10^{-4}$ , $N = 20,480$ . $K = L = 1024$ , $\mu c^2 = 1.2 \times 10^{-5}$	15
6. ALE output ROC curves for fixed filter length, $L$ , and varying DFT length $K$ . $P_{FA} = 10^{-4}$ . $L = 1024$ , $\mu c^2 = 4.1 \times 10^{-6}$ . $N = 102,400$	16

## INTRODUCTION

Several types of data adaptive detection structures\* have been proposed for use in environments where the signal and noise statistics are only vaguely known and where insufficient a priori information is available to design optimal detectors. Several types of adaptive mean level detectors have been implemented to provide improved performance over conventional nonadaptive systems when the noise statistics are nonstationary.<sup>1,2,3,4,5,6</sup> Other forms of adaptive receivers based on pattern recognition techniques, decision directed feedback, nonparametric statistics and sequential processing are described in References 7 through 14.

Adaptive implementations of linear prediction filters have recently been proposed for spectral analysis, instantaneous frequency estimation and speech encoding applications (References 15 through 20). A discussion of the properties and diverse applications of linear prediction filters is contained in Reference 21. The computational simplicity of adaptive linear prediction (ALP) implementations based on the Widrow-Hoff least mean squares (LMS) adaptive algorithm is discussed in References 15, 16, 17 and 18.

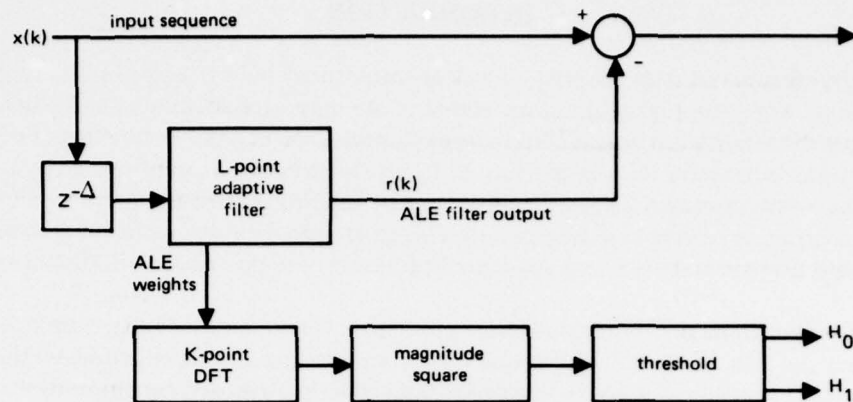
The application of LMS implementations of ALP filters to maximum entropy spectral analysis is described in References 15 and 18. The improved frequency resolution which is often attainable by the maximum entropy method (MEM) of spectral analysis is well documented in References 21 through 26. Baggeroer<sup>27</sup> has shown however that the high variance associated with inverting the quantity  $|1 - H(\omega)|^2$ , where  $H(\omega)$  is the transfer function of the linear predictive filter, can lead to increased confidence intervals for MEM estimates of sinusoidal components in noise.

It has been shown<sup>28</sup> that for multiple sinusoids in uncorrelated noise the magnitudes of the MEM frequency estimates at the sinusoidal frequencies degrade approximately as the square of the input signal-to-noise ratio (SNR) in the limit of large prediction filter lengths. Satorius and Zeidler<sup>29</sup> have shown further that the resolution attainable by MEM is frequency dependent when the sinusoids are embedded in an additive correlated noise background. Marple<sup>24</sup> has shown that the two-sinusoid resolution performance of MEM degrades as a function of input SNR to a resolution which is no better than that attainable by conventional spectral analysis techniques at low input SNR.

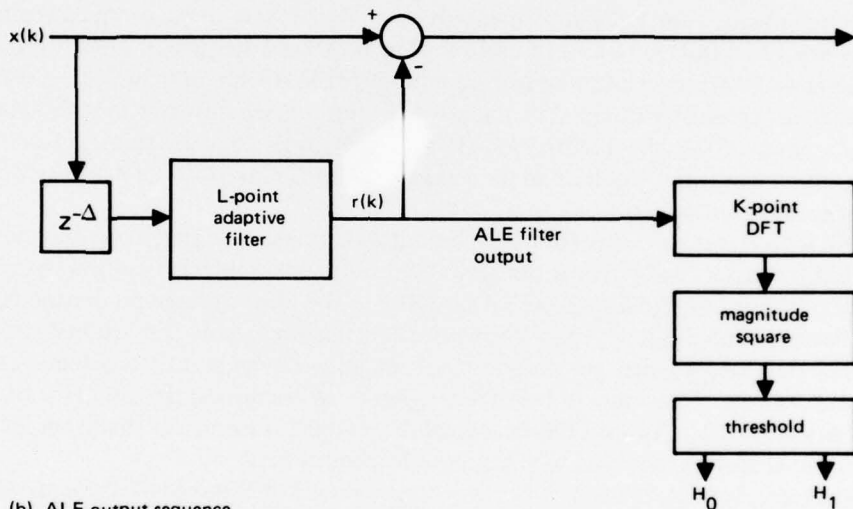
Alternate approaches to frequency estimation at low input SNR using an ALP as a prefilter to a conventional spectrum analyzer are discussed in References 16 and 17. In this case the ALP filter is used to estimate the frequencies at which coherent energy is present in the input data sequence and the spectrum analyzer examines the frequency content of either the adaptive filter weights or the adaptive filter output as illustrated in Figure 1. The ALP filter can be used to suppress either correlated or uncorrelated noise components of the input data by selecting the prediction distance ( $\Delta$  in Figure 1) on the basis of available a priori information concerning the expected autocorrelations of noise and signal components. Suppression of the additive noise prior to spectral analysis reduces the interference between the signal and noise components of the data before the spectral estimate is made. Appropriate selection of  $\Delta$  provides bandwidth selective spectral estimates.<sup>20</sup> This device has been called the adaptive line enhancer (ALE). The LMS algorithm provides a method for updating the ALP filter coefficients to track temporal variations in the signal and noise statistics.

---

\*An adaptive detection system is one in which the detector structure is based to some extent on the received data and which incorporates a mechanism to vary the detector structure as the received signal and noise characteristics evolve in time.



(a) ALE weight vector



(b) ALE output sequence

Figure 1. Adaptive detector implementations.

The detection performance of a data adaptive receiver in a nonstationary signal and noise environment is a difficult, if not intractable, problem.<sup>14</sup> The devices proposed in References 10 through 14 are not readily amenable to mathematical analysis and their performance generally has been defined empirically on the basis of computer simulation. In cases where the statistics of the signal and noise spectra evolve slowly in time, however, local stationarity can be invoked.<sup>21</sup> In these cases it is often possible to define optimal receiver configurations for the specified operating conditions. Steeson<sup>6</sup> and Dillard<sup>3</sup> discuss performance measures of an adaptive mean level detector relative to that of the optimal detector for specified stationary inputs as a function of the response time of the mean level detector.

Another performance criterion known as the asymptotic relative efficiency (ARE)<sup>30</sup> is sometimes used to evaluate the performance of an adaptive receiver.<sup>10,31</sup> The ARE is a comparative measure of the number of data samples required by a given detector to achieve the same detection probability and false alarm rate as the optimal detector for specified test

conditions. Nolte<sup>8,9</sup> has shown that for the case of detecting one-of-M known synchronous-recurrent transients in Gaussian uncorrelated noise, the optimal detector may be implemented through an adaptive sequential implementation.

For time-evolving noise and signal statistics an effective adaptive receiver must exhibit robust detection performance over the expected range of inputs statistics. Even in this case, however, performance analysis based on local stationarity assumptions gives baseline performance data for selecting desirable design parameters of adaptive detectors and/or estimators. For example, the ability of the ALE to estimate the frequency of a sinusoid in uncorrelated noise was shown to be dependent on the adaptive filter length and the adaptive time constant.<sup>16,17</sup> The estimation of the frequencies of multiple sinusoids in uncorrelated noise was shown to be dependent on  $\Delta$  as well.<sup>28</sup> Even more dramatic performance variations as a function of  $\Delta$  can be expected when operating in a correlated noise environment.

Using an analysis based on deflection statistics, comparative detection performance of both ALE implementations relative to that of a conventional nonadaptive detection system was considered by Burdic<sup>32</sup> for sinusoidal signals in both stationary and nonstationary white noise. There it is shown that both implementations of the ALE reduce the degradation in system performance due to variations in noise statistics. Reeves has derived receiver operating characteristic (ROC) detection curves of the ALE weight implementation for the signal known except for phase (SKEP) detection problem. (In the SKEP problem, the input signal is a sinusoid of known frequency and unknown phase in stationary white noise of known power.) Under the condition that the total length of the input data sequence, N, is much larger than L, Reeves compares the detection performance of the ALE weight implementation to that of the classical optimal detector and incoherently averaged DFTs of length L. The optimal detector is well-known<sup>14,36</sup> and may be shown to be an N-length coherent DFT which processes the entire N-length sequence. The results show that the detection performance of a single L-weight ALE detector evaluated at the N<sup>th</sup>-point of the input data sequence compares favorably with N/L incoherent averages of an L point DFT. In addition, a methodology was derived for defining optimal time constants of the ALE weight implementation.

This paper investigates the detection performance of the ALE output implementation for the SKEP detection problem and presents comparative performances of the two distinct ALE implementations for this case.

### ADAPTIVE LINE ENHANCER (ALE) PERFORMANCE FOR SINUSOIDAL INPUTS IN WHITE NOISE

As illustrated in Figure 1, the ALE consists of an L-tap linear prediction filter in which the filter coefficients are updated at the input sampling rate using the Widrow-Hoff LMS adaptive algorithm. The adaptive filter output  $r(k)$  is defined by

$$r(k) = \sum_{j=0}^{L-1} w_j(k)x(k-j-\Delta) \quad (1)$$

where  $\Delta$  is the prediction distance of the filter. The instantaneous estimation error is designated as  $e(k)$ , where  $e(k) = x(k) - r(k)$ . It has been shown<sup>16,28</sup> that the set of weight

coefficients which minimizes the expected (mean) square error,  $E[e^2(k)]$ , of the LMS adaptive filter can often be obtained from the discrete Wiener-Hopf matrix equation

$$R\mathbf{w}^* = \mathbf{P}. \quad (2)$$

In Equation 2,  $R$  is the  $L \times L$  autocorrelation matrix of the input sequence  $x(k)$ ,  $\mathbf{P}$  is the  $L \times 1$  cross-correlation vector with elements  $P_j = E[x(k)x(k+j+\Delta-1)]$  and the  $\mathbf{w}^*$  is the optimal least mean squares weight vector. The LMS algorithm is a gradient search method which iteratively seeks a solution to Equation 2 by updating each filter weight by the recursive relation

$$w_j(k+1) = w_j(k) + 2\mu e(k)x(k-j-\Delta) \quad (3)$$

where  $\mu$  is a feedback gain controlling stability and convergence of the algorithm. For uncorrelated stationary inputs, it has been shown<sup>16</sup> that the expected value of the  $w_j(k)$  in Equation 3 converges in the mean to the optimal  $w_j^*$  provided that  $\mu$  is bounded by  $0 < \mu < 1/\lambda_{\max}$  where  $\lambda_{\max}$  is the largest eigenvalue of the autocorrelation matrix  $R$ . Since the LMS algorithm approximates the true LMS error gradient with a finite data length estimate of the gradient, the weight vector coefficients thus are obtained from noisy estimates of the optimal Wiener filter solution. This gradient estimation noise is often called misadjustment noise and is given by  $V_j(k)$ , where

$$V_j(k) = w_j(k) - w_j^*. \quad (4)$$

Widrow et al<sup>16</sup> have shown that this excess error may be made arbitrarily small by decreasing the feedback parameter  $\mu$ . Decreasing  $\mu$  increases the convergence time of the LMS algorithm, however, and a compromise between the response time and the misadjustment noise power must be made in practical applications. Convergence properties of the algorithm for correlated stationary inputs in general are very difficult to derive analytically and a summary of results in this area is presented in Reference 28. In many practical applications involving correlated data, however, the expectation of  $w_j(k)$  converges within an excellent approximation to  $w_j^*$  provided  $\mu$  is sufficiently small.<sup>16</sup> Reference 28 has shown that experimentally obtained steady-state coefficients  $w_j(k)$  for inputs consisting of sinusoids in uncorrelated noise are in good agreement with the theoretical optimal coefficients  $w_j^*$ .

It is generally assumed<sup>16</sup> that the misadjustment noise is Gaussian distributed and uncorrelated from weight to weight. Further, it was shown for uncorrelated, stationary inputs that

$$E[V_j(k)] = 0 \quad (5a)$$

$$E[V_j(k)V_i(k)] = \mu c^2 \delta(i-j) \quad (5b)$$

where  $\delta(\cdot)$  is the Kronecker delta operator. Further it will be assumed that the variance of the misadjustment is essentially constant after the start of adaptation and is not dependent upon either signal presence or absence. Analytical solutions for  $w_j^*$  for a single sinusoid in uncorrelated noise have been derived by Triechler<sup>20</sup> and Reeves<sup>33</sup> for a sinusoid of known frequency  $\omega_0$  under the condition that

$$\frac{\omega_0 L}{2\pi} = \text{integer} \quad (6)$$

where  $\omega_0$  is normalized relative to the sampling frequency of  $2\pi$  radians. When Equation 6 is valid and the input is given by

$$x(k) = A \sin(\omega_0 k + \theta) + n(k) \quad (7)$$

where  $n(k)$  is a zero-mean white Gaussian noise sequence power  $v^2$ , the R matrix is circulant and it can readily be shown<sup>20,33</sup> that

$$w_j^* = \frac{2a^*}{L} \cos[\omega_0(j + \Delta)], \quad 0 \leq j \leq L-1 \quad (8)$$

In Equation 8,

$$a^* = \frac{(L/2)\text{SNR}}{1 + (L/2)\text{SNR}} \quad (9)$$

where SNR is the input signal-to-noise ratio defined as  $\text{SNR} = A^2/2v^2$ . Note that the amplitude of  $w_j^*$  depends nonlinearly on the input SNR. This effect is due to the difficulty in separating the narrowband and broadband components of  $x(k)$  near  $\omega_0$  at low SNR.  $w_j$  is defined in Reference 28 for a single sinusoid in white noise for the more general case in which R is not a circulant matrix. It is shown that Equation 8 also provides an excellent approximation to  $w_j$  for  $\pi/L < \omega_0 < \pi((L-1)/L)$  when R is not circulant.

Trinchler<sup>20</sup> has shown that the speed of adaptation of the LMS algorithm is controlled by the dominant eigenvalues of the R matrix. For the case of a single sinusoid in uncorrelated noise, the optimal weight vector is orthogonal to all eigenvectors of R except the conjugate pair of eigenvectors corresponding to frequency  $\omega_0$ . The eigenvalues associated with these eigenvectors dominate the convergence time and are both given by  $\lambda = v^2 + (A^2L/4)$ . As shown in Reference 20, when the filter is filled with data and all weights are zeroed at  $k=0$ , the mean value,  $\bar{w}_j(k)$ , of the  $j^{\text{th}}$  weight updates by the relation

$$\bar{w}_j(k) = [1 - (1 - 2\mu\lambda)^k] w_j^* ; k = 0, 1, \dots \quad (10)$$

When  $2\mu\lambda \ll 1$  and  $k \gg 1$ , Equation 10 reduces to

$$\bar{w}_j(k) = [1 - e^{-2\mu\lambda k}] w_j^* \quad (11)$$

In this case the mean adaptation time constant  $\tau_m$  is given by  $\tau_m = 1/2\mu\lambda$ . From Equations 8, 10 and 11, the dynamic solution for the adaptive filter weights is thus given in the mean by

$$\bar{w}_j(k) = \frac{2a(k)}{L} \cos[\omega_0(j + \Delta)], \quad 0 \leq j \leq L-1 \quad (12)$$

where

$$a(k) = [1 - e^{-k/\tau_m}] a^* \quad (13)$$

## DERIVATION OF DETECTION STATISTICS

### DETECTION STATISTICS FOR THE ALE OUTPUT DEVICE

The detection performance of the ALE filter output implementation will be analyzed under the condition that all adaptive filter weights are initialized to zero at  $k = 0$  and that the filter processes  $N$  data points prior to forming a detection statistic. The adaptive filter and the  $K$ -point DFT detector are restricted such that  $K$  and  $L$  are much less than  $N$ . The restriction that  $(K, L) \ll N$  eliminates initial transient behavior as the adaptive filter fills with data and allows the mean weight approximation given by Equation 12. Detection is based on a  $K$ -point DFT of the final  $K$  output values from the  $L$ -length filter and will be performed using the classical Neyman-Pearson hypothesis test. Two hypotheses,  $H_0$  and  $H_1$ , will be defined by  $H_0 : x(k) = n(k)$  and  $H_1 : x(k) = s(k | \theta) + n(k)$ . Here  $s(k | \theta)$  is the sinusoidal signal of known amplitude and frequency but unknown phase and  $n(k)$  is a sample of the Gaussian uncorrelated noise sequence with zero mean and variance  $v^2$ :

$$s(k | \theta) = A \sin(\omega_0 k + \theta) \quad , \quad (14)$$

$$E[n(k)n(p)] = v^2 \delta(k - p) \quad (15)$$

where  $v^2$  is known a priori.

In this section a detection statistic  $q$  will be defined for the ALE output device and the conditional probability density functions,  $p_0(q)$  and  $p_1(q)$  will be derived. The Neyman-Pearson criteria allows the probability of false alarm,  $P_{FA}$ , under  $H_0$  to be completely specified in terms of fixed threshold  $\beta_0$  such that if  $q \geq \beta_0$ , signal presence is declared, whereas if  $q < \beta_0$ , the decision of signal absence is made.

Since  $s(k | \theta)$  in Equation 14 is completely deterministic and zero-mean, the variable  $x(k)$  is a zero-mean Gaussian random variable for all values of  $k$ . The filter output conditioned on the unknown initial phase is thus defined by Equation 1. Further, since  $r(k | \theta)$  is a linear combination of previous input samples it is also a zero-mean Gaussian random variable. The output spectrum obtained from a  $K$ -point DFT of  $r(k | \theta)$  evaluated at  $\omega_0$  is given by  $R(\omega_0) = u + jv$ , where

$$\begin{aligned} u &= \sum_{k=0}^{K-1} r(k | \theta) \cos \omega_0 k, \\ v &= \sum_{k=0}^{K-1} r(k | \theta) \sin \omega_0 k \quad . \end{aligned} \quad (16)$$

The detection statistic  $q$  is then defined as<sup>14,36</sup>  $q = u^2 + v^2$ . The joint pdf for  $(u, v)$  must, therefore, be specified to define the pdf of the detection statistic  $q$ . Medaugh<sup>34</sup> has shown that  $u$  and  $v$  are essentially statistically independent for the signal and noise models assumed above for  $k \geq 4\tau_m$ . Since  $r(k | \theta)$  is a Gaussian random variable,  $u$  and  $v$  are also Gaussian and the pdf  $p(u, v)$  is written as

$$p(u,v) = [2\pi\sigma_u\sigma_v]^{-1} \exp \left\{ -\frac{1}{2} \left[ \left( \frac{u-\bar{u}}{\sigma_u} \right)^2 + \left( \frac{v-\bar{v}}{\sigma_v} \right)^2 \right] \right\} \quad (17)$$

where  $\bar{u}$  and  $\bar{v}$  are the component means and  $\sigma_u^2$  and  $\sigma_v^2$  are the component variances. The values of  $\bar{u}$ ,  $\bar{v}$ ,  $\sigma_u^2$ ,  $\sigma_v^2$  were derived for the steady-state adaptive filter response for equal DFT length and adaptive filter length ( $K=L$ ) in Reference 34 and extended for the case  $K \leq L$  in Reference 35. We will consider the ALE detection performance for  $K \leq L$ .

For  $\pi/L < \omega_0 < \pi[(L-1)/L]$ , the expressions for  $\bar{u}$  and  $\bar{v}$  are shown in Reference 35 to be closely approximated by

$$\bar{u} = a^*AK^2 \sin \theta/2L, \quad (18a)$$

$$\bar{v} = a^*AK^2 \cos \theta/2L \quad (18b)$$

Likewise, for low input SNR<sup>35</sup>

$$\sigma_u^2 = \sigma_v^2 = \frac{\mu c^2 v^2 LK}{2} + \frac{\mu c^2 A^2 LK^2}{8} + \frac{2a^{*2}v^2K^2}{L^2} \left( \frac{L}{4} - \frac{K}{12} \right) \quad (19)$$

where  $c^2$  is the total input power, signal plus noise. Note that in addition to raising the mean level of the  $\omega_0$  bin component as indicated by Equation 18, the presence of the signal markedly increases the variance of each DFT component through the appearance of  $A$  and  $a^*$  in Equation 19. (For the weight transform implementation, the variances of  $u$  and  $v$  are identical under  $H_0$  and  $H_1$ , Reference 33). The raising of the mean bin level through Equation 18 serves to shift  $p_1(q)$  higher on the  $q$  axis, while the larger variance will serve to broaden the pdf. These effects signify that  $p_1(q)$  is more highly skewed toward larger  $q$  values than is  $p_0(q)$ , thus enhancing detection over the case if  $p_1(q)$  were simply a mean-shifted replica of  $p_0(q)$ .

By ensuring that  $N \geq \tau_m$  and that  $(L,K) \ll N$ ,  $a^*$  in Equations 18 and 19 can be replaced by  $a(k)$  to describe the output statistics just prior to convergence. This signifies the means of Equation 18 build up exponentially with time constant  $\tau_m$  to their converged values, as shown by Triechler.<sup>20</sup> Thus, Equation 18 may be rewritten as

$$\bar{u} = \tilde{A} \sin \theta, \quad \bar{v} = \tilde{A} \cos \theta \quad (20a)$$

where

$$\tilde{A} = \frac{a(k)AK^2}{2L} \quad (20b)$$

Further, in this case the variance under  $H_1$  is now approximated by  $\sigma_1^2 = \sigma_u^2 = \sigma_v^2$ , where from Equation 19

$$\sigma_1^2 = \frac{\mu c^2 v^2 LK}{2} + \frac{\mu c^2 A^2 LK^2}{8} + \frac{2a^2(k)v^2K^2}{L^2} \left( \frac{L}{4} - \frac{K}{12} \right) \quad (21)$$

The first two components of  $\sigma_1^2$  are independent of time index  $k$  due to the assumption that the weight misadjustment noise is independent of  $k$  as defined by Equation 5. The first is due to the broadband weight misadjustment noise produced by the input white noise. The second component of  $\sigma_1^2$  is the weight misadjustment caused by presence

of the signal and is due to a narrowband noise process centered at frequency  $\omega_0$ . This narrowband noise process may be interpreted as adding a randomly-phased sinusoid with frequency  $\omega_0$  to the mean weight vector and the magnitude of this component defines the variance of the envelope of the sinusoid. The third component of the variance is due to the input white noise in the bandwidth of the adaptive filter and increases in magnitude with increasing  $k$  as the mean weight vector increases as defined by Equation 12. Note that the magnitude of this term is scaled by the convergence rate of the mean weight vector.

With  $\bar{u}$  and  $\bar{v}$  given by Equation 20 and  $\sigma_1^2$  given by Equation 21 the derivation of the pdfs for the detection variable  $q$  is straightforward<sup>14,36</sup> and is outlined in Appendix A. The results show that under  $H_0$ ,  $p_0(q)$  is the gamma density function with two degrees of freedom, given by

$$p_0(q) = \frac{1}{2\sigma_0^2} \exp \left[ -q/2\sigma_0^2 \right], \quad q \geq 0 \quad (22)$$

In Equation 22,  $\sigma_0^2$  is the variance of  $u$  and  $v$  under  $H_0$ , which is obtained from Equation 21 by setting  $A = 0$  and  $a^* = 0$ ; i.e.,  $\sigma_0^2 = \mu c^2 v^2 LK/2$ . Under  $H_1$ ,  $q$  has the density function  $p_1(q)$  given by

$$p_1(q) = \frac{1}{2\sigma_1^2} \exp \left[ -\frac{1}{2\sigma_1^2} (q + \tilde{A}^2) \right] I_0 \left( \frac{\tilde{A}q^{1/2}}{\sigma_1^2} \right), \quad q \geq 0, \quad (23)$$

where  $I_0(x)$  is the modified Bessel function of the first kind.

Following the Neyman-Pearson criteria, the  $P_{FA}$  is specified and used to obtain the threshold  $\beta_0$  under  $H_0$ :

$$\int_{\beta_0}^{\infty} p_0(q) dq = P_{FA} \quad (24)$$

where  $p_0(q)$  is given by Equation 22. Since  $P_{FA}$  and  $p_0(q)$  are known, Equation 24 completely specifies the threshold  $\beta_0$ . The probability of detection,  $P_D$ , is then simply the probability that the variable  $q$  exceeds this same threshold  $\beta_0$  when the signal is present, given by:

$$P_D = \int_{\beta_0}^{\infty} p_1(q) dq \quad (25)$$

with  $p_1(q)$  given by Equation 23.

A change of variables will transform the integrals in Equations 24 and 25 into more conventional forms. It may be shown<sup>36</sup> that equivalent forms of these integrals are

$$P_{FA} = \int_{T_0}^{\infty} \chi_2^2(p) dp \quad (26)$$

and

$$P_D = \int_{T_1}^{\infty} \chi_2^{2'}(p | \alpha) dp \quad (27)$$

where the notation  $\chi_2^2(p)$  is the chi-square pdf with 2 d.o.f. and  $\chi_2^{2'}(p | \alpha)$  is the non-central chi-square pdf with 2 d.o.f. and non-centrality parameter  $\alpha$ , where from Equations 20 and 21

$$\alpha = \frac{\tilde{A}^2}{\sigma_1^2} = \frac{K^3 a^2(k) \text{SNR} / \mu c^2 L^3}{1 + \frac{K}{2} \text{SNR} + \frac{4Ka^2(k)}{\mu c^2 L^3} \left( \frac{L}{4} - \frac{K}{12} \right)} \quad (28a)$$

Specification of  $P_{FA}$  in Equation 26 completely determines the threshold  $T_0$ . This threshold is then scaled by the ratio of the variances under  $H_0$  and  $H_1$  to define the threshold  $T_1$  by

$$T_1 = \left( \frac{\sigma_0}{\sigma_1} \right)^2 T_0 = \left[ \frac{1}{1 + \frac{K}{2} \text{SNR} + \frac{4Ka^2(k)}{\mu c^2 L^3} \left( \frac{L}{4} - \frac{K}{12} \right)} \right] T_0 \quad (28b)$$

The probability integrals Equations 26 and 27 may be evaluated by a non-numerical method developed by Urkowitz.<sup>37</sup>

#### DETECTION STATISTICS OF THE ALE WEIGHT VECTOR IMPLEMENTATION

Reeves<sup>33</sup> has examined the case of detection based on the ALE weight vector implementation for the SKEP problem. Detection is based upon thresholding a random variable defined to be the magnitude-square of the  $\omega_0$ -component of the L-point DFT of the final weight vector. Reeves assumes that the mean ALE weights are described by Equation 12 and that Equation 7 is also a valid description of misadjustment noise. These lead to a derivation<sup>33</sup> of integrals which have the forms

$$P_{FA} = \int_{T_0}^{\infty} \chi_2^2(z) dz \quad (29)$$

and

$$P_D = \int_{T_0}^{\infty} \chi_2^{2'}(z | \alpha_w) dz \quad (30)$$

where  $\alpha_w = a^2(k) / \sigma_w^2$ , and  $\sigma_w^2$  is one-half the real weight variance of the  $\omega_0$ -component, derivable from Reference 16 as  $\sigma_w^2 = \mu c^2 L / 2$ . Note that the thresholds in each integral are  $T_0$ , due to equal variance of the weight vector detection statistic under  $H_0$  and  $H_1$ . The

integrals Equations 29 and 30 may also be non-numerically evaluated by the methods outlined in Appendix B.

### DETECTION STATISTICS FOR INCOHERENTLY AVERAGED DFT PROCESSOR

For this commonly used processor, the N-length input sequence is divided into M blocks of K-points each and a coherent K-point DFT is formed for each block. The block DFTs are then averaged, forming the detection statistic u (normalized to unity variance), which is the magnitude square of the  $\omega_0$  component. The statistic u under  $H_0$  has been shown to be<sup>33,36</sup> the chi-squared density function with 2M degrees of freedom due to the 2M random variables added together to form u. This defines the threshold  $\beta_0$  by the integral relationship

$$P_{FA} = \int_{\beta_0}^{\infty} \chi_{2M}^2(u) du \quad (31)$$

Under  $H_1$ , the detection statistic u has the non-central chi-squared density function with 2M degrees of freedom and non-centrality parameter  $\alpha_1$ , where  $\alpha_1 = N$  (SNR) from Reference 33. Since the statistical variance on u is not dependent upon signal presence or absence, the threshold under  $H_1$  is equal to  $\beta_0$  giving the following expression for  $P_D$ :

$$P_D = \int_{\beta_0}^{\infty} \chi_{2M}'(u | \alpha_1) du \quad (32)$$

The threshold  $\beta_0$  in Equation 31 and the evaluation of  $P_D$  in Equation 32 may be found by the methods presented in Appendix B.

### PERFORMANCE ANALYSIS

The detection performance of the adaptive implementations and the conventional DFT processor of the previous section will be compared on the basis of ROC analysis. A value of  $P_{FA}$  is specified and held constant for a set of hypotheses tests, while the input signal strength is varied. The results are sets of curves which give  $P_D$  as a function of input SNR for different processor configurations.

There is a fundamental tradeoff in selecting appropriate adaptive filter time constants since reducing  $\mu$  decreases the misadjustment noise power as indicated by Equation 5, but correspondingly increases convergence time as indicated by Equation 11. Reeves has shown that there is an optimal value of  $\mu$  which maximizes the probability of detection at specified values of N, L and SNR for the ALE weight implementation. Assuming a low input SNR ( $c^2 \cong v^2$ ) and that detection is based on the last weight vector ( $k = N$ ), the optimal value of  $\mu$  was shown to be:

$$\mu_0 = \frac{1.25643}{2c^2N(1 + \frac{L}{2} \hat{SNR})} \quad (33)$$

where  $\hat{SNR}$  is a nominal input SNR which may be expected at the receiver input and the numerator of Equation 33 is the non-trivial root of the transcendental equation  $(1 + 2x)e^{-x} = 1$ . Reeves has shown that detector performance is not strongly influenced by choice of SNR. Medaugh<sup>38</sup> has similarly investigated the optimality of  $\mu$  for detection based on filter output for the case  $K = L$  and found the same expression as Equation 33 gives the optimal  $\mu$ . These results may be easily extended to the case for  $K \leq L$  by simultaneously maximizing the non-centrality parameter  $\alpha$  and minimizing the threshold scaling factor  $(\sigma_0^2/\sigma_1^2)$ , both given in Equation 28, with respect to  $\mu$ . By taking partial derivatives of  $\alpha$  and  $(\sigma_0/\sigma_1)^2$  with respect to  $\mu$  and equating to zero, it may be shown that  $\mu_0$  as defined by Equation 33 is equivalently the optimal  $\mu$  for detection based on filter output with  $K \leq L$ .

An important property of the ALE is the relative insensitivity of the adaptive filter to its feedback gain parameter  $\mu$ . While there is an optimal  $\mu$  value for a given fixed set of parameters, detection performance of either ALE implementation is not critically dependent upon  $\mu$ , as seen from Figure 2. In this figure, the SNR at which  $P_D$  equals 50 percent has been plotted as a function of  $\mu$  for both processors for some typical parameters. The  $P_{FA}$  was held constant at  $10^{-4}$ . The shape of the curves for each implementation is consistent for both filter lengths and the broad minima show that near-optimal (with respect to  $\mu$ ) performance may be obtained for a wide range of  $\mu$  settings.

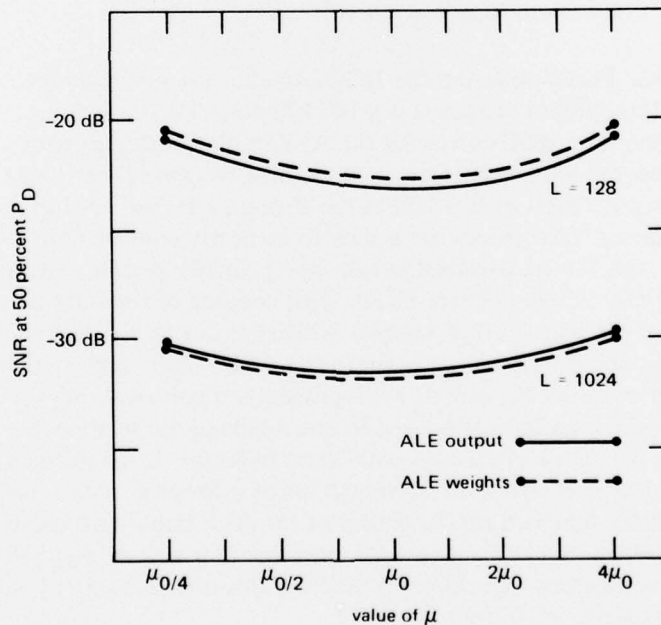


Figure 2. SNR at 50 percent  $P_D$  as a function of optimal  $\mu_0$ .  $K = L$ ,  $P_{FA} = 10^{-4}$ .

Figure 3 displays  $P_D$  versus input SNR for the case  $K = L = 1024$  and an input data

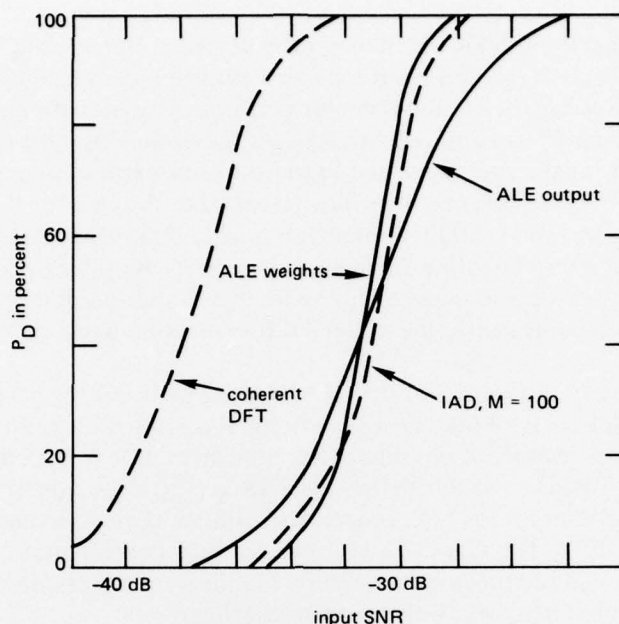


Figure 3. ROC curves for  $P_{FA} = 10^{-4}$ ,  $N = 102,400$ .  
 $K = L = 1024$ ,  $\mu c^2 = 4.1 \times 10^{-6}$ .

sequence of  $N = 100L$ . For comparison the ROC curve for the optimal processor for this case is also shown. The optimal processor is a 102400-point DFT which processes the entire data record coherently. The ROC curves for the ALE implementations with  $\mu$  chosen by Equation 33 are compared with that of the incoherently averaged DFT (IAD) processor which ensemble averages a total of  $M = 100$  of the  $K$ -point DFTs of the input sequence. Performance of the latter three processors is seen to be nearly equivalent in the vicinity of  $P_D = 50$  percent, with the ALE output device giving slightly poorer performance at higher SNRs, but slightly better at lower SNRs. This bending of the output curve is caused by the components of the filter output variance which are due to signal presence, as shown by Equation 21. This behavior does not occur in the ALE weight device or the IAD processor since the variances under  $H_0$  and  $H_1$  are equivalent. Figure 4 shows the case for shortening the filter and DFT lengths to  $K = L = 128$  but retaining the relation  $N = 100L$ . The general shapes of the curves are consistent with those in Figure 3; the primary difference is in raising the detectable SNR levels, reflecting the lower number of data samples used. Figures 3 and 4 together demonstrate the ability of the ALE implementations to maintain consistent detection characteristics over a wide range of filter lengths and SNRs, providing the ratio  $N/L$  remains constant. The effect of altering this ratio is seen in Figure 5, which gives performance for  $K = L = 1024$  and  $N = 20L$ .

Another important result of adaptive prefiltering may be seen in Figure 6, in which filter length  $L$  has been held constant at  $L = 1024$  and  $K$  has been varied over a wide range such that  $K \leq L$ . As  $K$  decreases, performance degrades only slightly and asymptotically

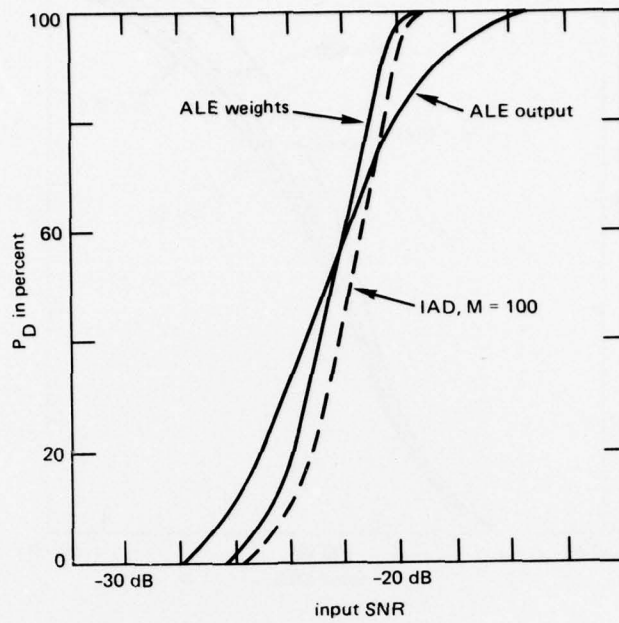


Figure 4. ROC curves for  $P_{FA} = 10^{-4}$ ,  $N = 12,800$ .  
 $K = L = 128$ ,  $\mu c^2 = 3 \times 10^{-5}$ .

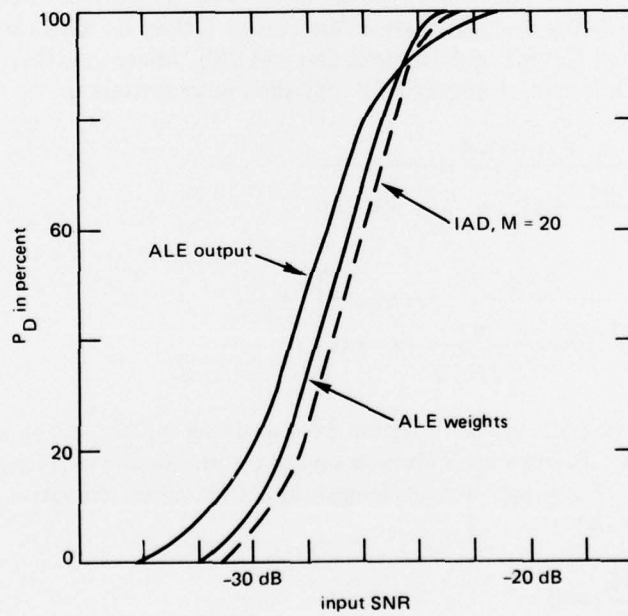


Figure 5. ROC curves for  $P_{FA} = 10^{-4}$ ,  $N = 20,480$ .  
 $K = L = 1024$ ,  $\mu c^2 = 1.2 \times 10^{-5}$ .

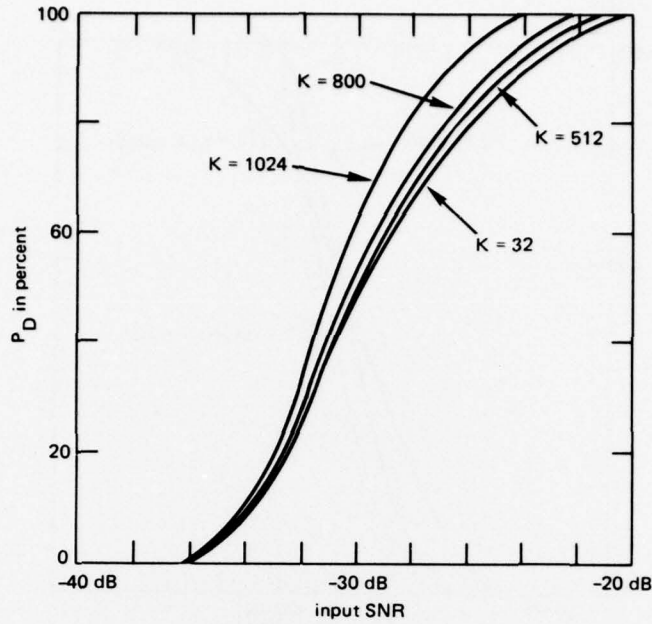


Figure 6. ALE output ROC curves for fixed filter length,  $L$ , and varying DFT length,  $K$ .  $P_{FA} = 10^{-4}$ .  $L = 1024$ ,  $\mu c^2 = 4.1 \times 10^{-6}$ .

approaches an ROC curve which is independent of  $K$ . This is due to the detection statistic distribution under  $H_1$  being more strongly a function of  $L$  than  $K$ . This can be seen by making the substitution  $K = mL$  in Equations 28a and 28b, where  $m$  is the fraction ( $m \leq 1$ ) relating DFT and ALE length. Equations 28 may then be rewritten as:

$$\alpha = \frac{m^3 a^2(k) \text{SNR}}{\mu c^2 \left(1 + \frac{mL}{2} \text{SNR}\right) + \frac{ma^2}{3L} (3 - m)} \quad (34a)$$

$$T_I = \left[ \frac{1}{1 + \frac{mL}{2} \text{SNR} + \frac{ma^2}{3\mu c^2 L} (3 - m)} \right] T_O \quad (34b)$$

Now let  $m$  approach zero in Equation 34, signifying shorter and shorter DFTs with respect to ALE length. Performing a limiting operation produces a unit-length (one-point) DFT, giving  $m = L^{-1}$ . For practical filter lengths and SNR values, Equations 34 then are closely approximated by:

$$\alpha = \frac{a^2(k) \text{SNR}}{\mu c^2 L^3} \cong 0 \quad (35a)$$

$$T_1 = \left[ \frac{1}{1 + a^2(k)/\mu c^2 L^2} \right] T_0 \quad (35b)$$

From Equation 35a it is seen that the non-centrality parameter,  $\alpha$ , approaches zero as  $K$  is taken to its lower limit. However, from Equation 35b it is seen that there is still an appreciable threshold reduction under  $H_1$ , which is entirely a function of the adaptive filter parameters. The fraction  $a^2(k)/\mu c^2 L^2$  has an appreciable magnitude for a wide range of filter parameters, thus providing the reduced threshold  $T_1$  and the resultant gain in detection. Using an adaptive filter length of  $L = 1024$ , detection ROC curves for  $K = 1024, 800, 512$  and  $32$  are shown in Figure 6. The limiting cases of Equations 35 are approached quickly, as can be seen from the closeness of the curves for  $K = 512$  and  $K = 32$ .

### SUMMARY

This paper has examined the detection properties of two adaptive detector implementations for the SKEP problem. Detection performances by ROC analysis for the  $L$ -tap ALE weight vector and filter output devices using  $K$ -point DFTs and processing  $N$ -length data sequences have been shown to be roughly equivalent to incoherent averaging of an  $L$ -point DFT for a wide range of  $K, L$  and  $N$ . The specific differences between detection properties of each ALE implementation have been described and shown to be due to the different variance characteristics of each processor. The detection performance of the ALE processors has been shown to be relatively insensitive to the choice of adaptive feedback constant  $\mu$ . Finally, detection performance for the two ALE implementations was also shown to be not crucially dependent upon DFT detector length  $K$ .

## REFERENCES

1. J.T. Rickard and G.M. Dillard, "Adaptive Detection Algorithms for Multiple Target Situations." IEEE Transactions on Aerospace and Electronic Systems, AES-13, pp. 338-44, 1977.
2. D.J. Gupta, J.F. Vetelino, T.J. Curry and J.T. Francis, "An Adaptive Threshold System for Nonstationary Noise Backgrounds." IEEE Transactions on Aerospace and Electronic Systems, AES-13, pp. 11-16, 1977.
3. G.M. Dillard, "Mean Level Detection of Nonfluctuating Signals." IEEE Transactions on Aerospace and Electronic Systems, AES-10, pp. 795-79, 1974.
4. Ramon Nitzberg, "Constant False Alarm Rate Processors for Locally Nonstationary Clutter." IEEE Transactions on Aerospace and Electronic Systems, AES-9, pp. 399-406, 1972.
5. Ramon Nitzberg, "Constant False Alarm Rate Signal Processors for Several Types of Interference." IEEE Transactions on Aerospace and Electronic Systems, AES-8, pp. 27-35, 1972.
6. B.O. Steeson, "Detection Performance of a Mean Level Threshold." IEEE Transactions on Aerospace and Electronic Systems, AES-4, pp. 529-535, 1968.
7. E.J. Baxa and L.W. Nolte, "Adaptive Signal Detection with Finite Memory." IEEE Transactions on Systems, Man and Cybernetics, 2, p. 42, 1972.
8. L.W. Nolte, "Theory of Signal Detectability: Adaptive Optimum Receiver Design." Journal of the Acoustical Society of America, 42, p. 773, 1967.
9. L.W. Nolte, "Adaptive Optimum Detection: Synchronous Recurrent Transients." Journal of the Acoustical Society of America, 44, p. 224, 1968.
10. H.L. Groginsky, L.R. Wilson and David Middleton, "Adaptive Detection of Signals in Noise." Transactions IEEE, IT-12, 337, 1966.
11. H.J. Scudder III, "Adaptive Communications Receivers." Transactions IEEE, IT-11, 167, 1965.
12. N. Abramson and D. Braverman, "Learning to Recognize Patterns in a Random Environment." Transactions IRE IT-8, S58, 1962.
13. E.M. Glaser, "Signal Detection by Adaptive Filters." Transactions IRE IT-7, 87, 1961.
14. C.W. Helstrom, Statistical Theory of Signal Detection. Pergamon Press, Oxford, 1975.
15. L.J. Griffiths, "Rapid Measurement of Digital Instantaneous Frequency." IEEE Transactions on Acoustics, Speech and Signal Processing, ASSP-23, p. 209, 1972.
16. Bernard Widrow, et. al, "Adaptive Noise Cancelling Principles and Applications." Proceedings of IEEE, 63, 1962, 1975.

17. J.R. Zeidler and D.M. Chabries, "An Analysis of the LMS Adaptive Filter Used as a Spectral Line Enhancer." Naval Undersea Center, San Diego, NUC TP 556, February 1975.
18. D.R. Morgan and S.E. Craig, "Real Time Linear Prediction Using the Least Mean Squares Adaptive Algorithm." IEEE Transactions on Acoustics, Speech and Signal Processing, ASSP-24, 494, 1976.
19. R.J. Keeler and L.J. Griffiths, "Acoustic Doppler Extraction by Adaptive Linear Filtering." Journal of the Acoustical Society of America, 61, 1812, 1977.
20. J.R. Treichler, "The Spectral Line Enhancer – the Concept, an Implementation and an Application." Ph.D. dissertation, Department of Electrical Engineering, Stanford University, Stanford, CA, 1977.
21. John Makhoul, "Linear Prediction: A Tutorial Review." Proceedings of IEEE, 63, 561, 1975.
22. T.J. Ulrych and T.N. Bishop, "Maximum Entropy Spectral Analysis and Autoregressive Decomposition." Review of Geophysics and Space Physics, 33, 183, 1975.
23. T.J. Ulrych and R.W. Clayton, "Time Series Modelling and Maximum Entropy." Physics of the Earth and Planetary Interiors, 12, 188, 1976.
24. S.L. Marple, "Conventional Fourier Autoregressive and Special ARMA Methods of Spectrum Analysis." Engineer's Degree thesis, Department of Electrical Engineering, Stanford University, Stanford, CA, 1976.
25. J.P. Burg, "Maximum Entropy Spectral Analysis," Ph.D. dissertation, Department of Geophysics, Stanford University, Stanford, CA, 1975.
26. R.T. Lacoss, "Data Adaptive Spectral Analysis Methods." Geophysics, 36, 661, 1971.
27. A.B. Baggeroer, "Confidence Intervals for Regression (MEM) Spectral Estimates." IEEE Transactions on Information Theory, IT-22, p. 534, 1976.
28. J.R. Zeidler, E.H. Satorius, D.M. Chabries, H. Wexler, "Adaptive Enhancement of Multiple Sinusoids in Uncorrelated Noise." Naval Ocean Systems Center, San Diego. Accepted for publication in IEEE Transactions on Acoustics, Speech and Signal Processing.
29. E.H. Satorius and J.R. Zeidler, "Maximum Entropy Spectral Analysis of Multiple Sinusoids in Noise." Naval Ocean Systems Center, San Diego. Accepted for publication in Geophysics.
30. Jack Capon, "On Asymptotic Relative Efficiency of Locally Optimal Detectors." IRE Transactions on Information Theory, IT-7, pp. 67-71, 1961.
31. M.N. Woinsky, "Nonparametric Detection Using Spectral Data." IEEE Transactions on Information Theory, IT-18, pp. 110-118, 1972.

32. W.S. Burdic, "Detection of Narrowband Signals Using Time Domain Adaptive Filters." Autonetics Group, Rockwell International, Anaheim, CA. To be published.
33. P.M. Reeves, "Detection of Sinusoids in White Noise by Linear Predictive Filters." Naval Ocean Systems Center, San Diego. To be published.
34. L.J. Griffiths, Jeffrey Keeler, Raymond Medaugh, "Detection and Convergence Results Relating to the Performance of an Adaptive Line Enhancer ." Naval Undersea Center, San Diego, NUC TN 1831, December 1976.
35. S.T. Alexander, "The ALE Output Covariance Function for a Sinusoid in Uncorrelated Noise." Naval Ocean Systems Center, San Diego, NOSC TR 162, 1 Aug 1977.
36. A.D. Whalen, Detection of Signals in Noise. Academic Press, New York, 1971.
37. Harry Urkowitz, "Energy Detection of Unknown Deterministic Signals." Proceedings of IEEE, Volume 55, Number 4, April 1967.
38. L.J. Griffiths and Raymond Medaugh, "Optimal Adaptive Step Size Values for Detection Based on ALE Output." University of Colorado, Department of Electrical Engineering, Contract Report N00953-77-C-0008, July 15, 1977.

**APPENDIX A**  
**DERIVATION OF PDFs FOR ALE FILTER OUTPUT**

From Equation 17, the joint pdf for the random variables  $u$  and  $v$  is specified in terms of their means and variances under  $H_1$ . The output statistic  $q$  has been defined as the sum of the squares of  $u$  and  $v$ :

$$q = u^2 + v^2 \quad (A1)$$

and thus it is necessary to make the transformation of variables to obtain the pdfs of  $q$  from the joint pdf of  $(u,v)$ . This transformation is straightforward and follows the development in Whalen.\*

First, the pdf of random variable  $q$  under  $H_1$ , denoted  $p_1(q)$ , will be derived and a simple modification to  $p_1(q)$  will allow us to find easily the pdf of  $q$  under  $H_0$ , denoted  $p_0(q)$ . Thus, from Equation 17

$$p_1(u,v) = \frac{1}{2\pi\sigma_u\sigma_v} \exp \left[ -\frac{1}{2} \left( \frac{u - \bar{u}}{\sigma_u} \right)^2 - \frac{1}{2} \left( \frac{v - \bar{v}}{\sigma_v} \right)^2 \right] \quad (A2)$$

From Equation 19, it is seen that

$$\sigma_u^2 = \sigma_v^2 = \sigma_1^2$$

and from Equation 20 the component means under  $H_1$  are given by

$$\bar{u} = \tilde{A} \sin \theta \quad (A3)$$

$$\bar{v} = \tilde{A} \cos \theta \quad (A4)$$

Using these relations, the joint pdf for  $(u,v)$  given  $\theta$ , denoted by  $p_1(u,v | \theta)$ , becomes

$$p_1(u,v | \theta) = \frac{1}{2\pi\sigma_1^2} \exp \left\{ -\frac{1}{2\sigma_1^2} \left[ u^2 + v^2 + \tilde{A}^2 - 2A(u \sin \theta + v \cos \theta) \right] \right\} \quad (A5)$$

Now make the intermediate change of variables

$$v = z \cos \psi, \quad u = z \sin \psi \quad (A6)$$

This will allow Equation A5 to be transformed from the  $u,v$  coordinates to the  $z,\psi$  coordinates by the transformation\*

$$p_1(z,\psi | \theta) = |J| p_1(u,v | \theta) \begin{cases} u = f(z,\psi) \\ v = g(z,\psi) \end{cases}$$

where  $|J|$  is the determinant of the Jacobian for  $z$  and  $\psi$  and is given by

\*A.D. Whalen, Detection Signals in Noise. Academic Press, New York, 1971.

$$|J| = \begin{vmatrix} \frac{\partial v}{\partial z} & \frac{\partial u}{\partial z} \\ \frac{\partial v}{\partial \psi} & \frac{\partial u}{\partial \psi} \end{vmatrix}$$

For these variables,  $|J| = z$  and thus, by using a trigonometric identity, Equation A5 becomes

$$p_1(z, \psi | \theta) = \frac{z}{2\pi\sigma_1^2} \exp \left\{ -\frac{1}{2\sigma_1^2} \left[ z^2 + \tilde{A}^2 - 2\tilde{A}z \cos(\theta - \psi) \right] \right\}$$

The dependence on the dummy variable  $\psi$  may be removed by integrating over the range of  $\psi$ :

$$\begin{aligned} p_1(z | \theta) &= \int_0^{2\pi} p_1(z, \psi | \theta) d\psi \\ &= \frac{z}{2\pi\sigma_1^2} \exp \left[ -\frac{1}{2\sigma_1^2} (z^2 + \tilde{A}^2) \right] \int_0^{2\pi} \exp \left[ \frac{\tilde{A}z}{\sigma_1^2} \cos(\theta - \psi) \right] d\psi \quad (A7) \end{aligned}$$

The integral in Equation A7 is well known to be

$$\int_0^{2\pi} \exp \left[ \frac{\tilde{A}z}{\sigma_1^2} \cos(\theta - \psi) \right] d\psi = 2\pi I_0 \left( \frac{\tilde{A}z}{\sigma_1^2} \right)$$

where  $I_0(x)$  is the modified Bessel function of order zero. Thus the pdf of the statistic  $z$  is no longer dependent upon  $\theta$  and is given by

$$p_1(z) = \frac{z}{\sigma_1^2} \exp \left[ -\frac{1}{2\sigma_1^2} (z^2 + \tilde{A}^2) \right] I_0 \left( \frac{\tilde{A}z}{\sigma_1^2} \right) \quad (A8)$$

One more change of variable must be made. From Equation A6 it is seen that  $z^2 = u^2 + v^2$ , which is exactly equal to the detection statistic  $q$  as defined by Equation A1. Thus the pdf of the desired statistic  $q$  may be obtained by the transformation

$$p_1(q) = \left| \frac{\partial z}{\partial q} \right| p(z) \Big|_{z=f(q)}$$

In this transformation,  $z = q^{1/2}$  and Equation A8 becomes

$$p_1(q) = \frac{1}{2\sigma_1^2} \exp \left[ -\frac{1}{2\sigma_1^2} (q + \tilde{A}^2) \right] I_0 \left( \frac{\tilde{A}q^{1/2}}{\sigma_1^2} \right), \quad q \geq 0 \quad (A9)$$

Equation A9 is the pdf of the desired detection statistic  $q$  under  $H_1$ . The pdf of  $q$  under  $H_0$ , the hypothesis of no signal present, is easily obtained from Equation A9 by observing that for no signal present,  $\tilde{A} = 0$  from Equation 20b and the variance becomes  $\sigma_0^2$  as defined in Equation 22. The pdf of  $q$  under  $H_0$ ,  $p_0(q)$ , results from substituting these values into Equation A9, giving

$$p_0(q) = \frac{1}{2\sigma_0^2} \exp \left[ -q/2\sigma_0^2 \right] , \quad q \geq 0 \quad (\text{A10})$$

since  $I_0(0) = 1$ .

**APPENDIX B  
EVALUATION OF PROBABILITY INTEGRALS**

To determine the detection performance of the processors mentioned in this paper, it is necessary to evaluate two integrals of the forms:

$$P_{FA} = \int_{T_0}^{\infty} \chi_F^2(r) dr \quad (B1)$$

$$P_D = \int_{T_1}^{\infty} \chi_F^2(r | \alpha) dr \quad (B2)$$

In Equation B1,  $\chi_F^2(r)$  is the chi-square probability density function with F degrees of freedom given by Reference 36 in the main text:

$$\chi_F^2(r) = \frac{r^{(F-2)/2}}{2^{F/2} \Gamma(F/2)} \exp[-r/2] \quad , \quad r \geq 0 \quad (B3)$$

where  $\Gamma(F/2)$  is the gamma function which for integer values of  $(F/2)$  may be replaced by  $(F/2)!$ . In Equation B2,  $\chi_F^2(r | \alpha)$  is the non-central chi-square pdf with F degrees of freedom and non-centrality parameter  $\alpha$ , given by

$$\chi_F^2(r | \alpha) = \frac{1}{2} \left( \frac{r}{\alpha} \right)^{(F-2)/4} \exp \left\{ -\frac{r}{2} - \frac{\alpha}{2} \right\} I_{(F-2)/2}(\sqrt{r\alpha}) \quad , \quad r \geq 0 \quad (B4)$$

Consider first Equation B1, which is used to determine the threshold,  $T_0$ , under  $H_0$ . For  $F = 2$ , it is seen that the integral in Equation B1 may be evaluated immediately to give the relation

$$T_0 = -2 \ln P_{FA} \quad (B5)$$

For  $F > 2$ , however, direct integration of Equation B1 becomes quite tedious. Fortunately, Urkowitz\*\* has developed a nomographic method for determining  $T_0$ , given  $P_{FA}$  and F, and its use is straightforward. This method is accurate for  $F \leq 200$ , but for  $F > 200$ , the pdf  $\chi_F^2(r)$  is essentially Gaussian and the following approximation is valid:\*\*

$$P_{FA} \cong \frac{1}{2} \operatorname{erfc} \left[ \frac{T_0 - F}{2\sqrt{F}} \right] \quad (B6)$$

where  $\operatorname{erfc}(z)$  is the complementary error function, given by

$$\operatorname{erfc}(z) = \frac{2}{\sqrt{\pi}} \int_z^{\infty} \exp(-x^2) dx \quad (B7)$$

\*A.D. Whalen, Detection Signals in Noise. Academic Press, New York, 1971.

\*\*Harry Urkowitz, "Energy Detection of Unknown Deterministic Signals." Proceedings of IEEE, Volume 55, Number 4, April 1967.

This function has been extensively evaluated and appears in many references\*.

Now consider the integral in Equation B2. The evaluation of  $P_D$  requires that the non-central chi-square pdf be integrated from a known threshold  $r = T_1$  to  $r = \infty$ . This is equivalent to finding the quantity

$$P_D = 1 - \int_{-\infty}^{T_1} \chi_F^2(r|\alpha) dr \quad (B8)$$

where the second term of the right-hand side of Equation B8 is recognized to be the non-central chi-square cumulative distribution function evaluated at  $r = T_1$ . Urkowitz has shown that this function may be made equivalent (through appropriate choice of arguments) to the incomplete Toronto function\*\* for which tabulated curves are available. The incomplete Toronto function is defined by

$$T_{B(m,n,p)} = 2p^{n-m+1} e^{-p^2} \int_0^B t^{m-n} e^{-t^2} I_n(2pt) dt \quad (B9)$$

Using Equations B4, B8 and B9 and the relations

$$\begin{aligned} T_1 &= 2B^2 \\ m &= F - 1 \\ n &= (F-2)/2 \\ p^2 &= \alpha/2 \end{aligned} \quad (B10)$$

One may show that the probability of detection  $P_D$  is given by

$$P_D = 1 - T_{\sqrt{T_1}/2}(F-1, F/2-1, \sqrt{\alpha/2}) \quad (B11)$$

Curves for the incomplete Toronto function for a number of values of  $F$  are given in Marcum\*\*, but it is often desired to calculate  $P_D$  for degrees of freedom other than those selected in Marcum. An example of this is the case of incoherent averaging, in which  $F/2$  uncorrelated statistics with two degrees of freedom are summed to produce the final detection statistic with  $F$  degrees of freedom. In this case,  $F$  may be too large to be useful in the above method. However, Urkowitz has developed a nomographic method to evaluate  $P_D$  in such cases. This method is valid for  $F \leq 200$  and for  $F > 200$ , the Gaussian approximation may be employed which produces the following approximation for  $P_D$ :

$$P_D = \frac{1}{2} \operatorname{erfc} \left[ \frac{T_1 - F - \alpha}{2\sqrt{F + 2\alpha}} \right] \quad (B12)$$

\*M. Abramovitz and J.A. Stegun, eds., Handbook of Mathematical Functions, NBS Applied Mathematics, Series 55. USGPO, Washington, D.C., 1964.

\*\*J.I. Marcum, "A Statistical Theory of Target Detection by Pulsed Radar." IRE Transactions on Information Theory, Volume IT-6, April 1960.